NASA/CR-2002-211953
ICASE Report No. 2002-41

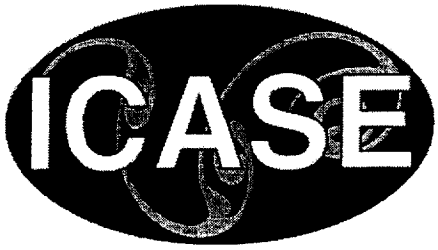


# The Stress-strain Behavior of Polymer-nanotube Composites from Molecular Dynamics Simulations

*S.J.V. Frankland, V.M. Harik, and G.M. Odegard*
*ICASE, Hampton, Virginia*

*D.W. Brenner*
*North Carolina State University, Raleigh, North Carolina*

*T.S. Gates*
*NASA Langley Research Center, Hampton, Virginia*


November 2002

## The NASA STI Program Office . . . in Profile

Since its founding, NASA has been dedicated to the advancement of aeronautics and space science. The NASA Scientific and Technical Information (STI) Program Office plays a key part in helping NASA maintain this important role.

The NASA STI Program Office is operated by Langley Research Center, the lead center for NASA's scientific and technical information. The NASA STI Program Office provides access to the NASA STI Database, the largest collection of aeronautical and space science STI in the world. The Program Office is also NASA's institutional mechanism for disseminating the results of its research and development activities. These results are published by NASA in the NASA STI Report Series, which includes the following report types:

- TECHNICAL PUBLICATION. Reports of completed research or a major significant phase of research that present the results of NASA programs and include extensive data or theoretical analysis. Includes compilations of significant scientific and technical data and information deemed to be of continuing reference value. NASA's counterpart of peer-reviewed formal professional papers, but having less stringent limitations on manuscript length and extent of graphic presentations.

- TECHNICAL MEMORANDUM. Scientific and technical findings that are preliminary or of specialized interest, e.g., quick release reports, working papers, and bibliographies that contain minimal annotation. Does not contain extensive analysis.

- CONTRACTOR REPORT. Scientific and technical findings by NASA-sponsored contractors and grantees.

- CONFERENCE PUBLICATIONS. Collected papers from scientific and technical conferences, symposia, seminars, or other meetings sponsored or cosponsored by NASA.

- SPECIAL PUBLICATION. Scientific, technical, or historical information from NASA programs, projects, and missions, often concerned with subjects having substantial public interest.

- TECHNICAL TRANSLATION. English-language translations of foreign scientific and technical material pertinent to NASA's mission.

Specialized services that complement the STI Program Office's diverse offerings include creating custom thesauri, building customized data bases, organizing and publishing research results . . . even providing videos.

For more information about the NASA STI Program Office, see the following:

- Access the NASA STI Program Home Page at ***http://www.sti.nasa.gov***

- Email your question via the Internet to help@sti.nasa.gov

- Fax your question to the NASA STI Help Desk at (301) 621-0134

- Telephone the NASA STI Help Desk at (301) 621-0390

- Write to:
  NASA STI Help Desk
  NASA Center for AeroSpace Information
  7121 Standard Drive
  Hanover, MD 21076-1320

NASA/CR-2002-211953
ICASE Report No. 2002-41

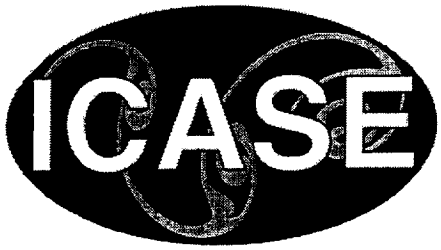


# The Stress-strain Behavior of Polymer-nanotube Composites from Molecular Dynamics Simulations

*S.J.V. Frankland, V.M. Harik, and G.M. Odegard*
*ICASE, Hampton, Virginia*

*D.W. Brenner*
*North Carolina State University, Raleigh, North Carolina*

*T.S. Gates*
*NASA Langley Research Center, Hampton, Virginia*

*ICASE*
*NASA Langley Research Center*
*Hampton, Virginia*
*Operated by Universities Space Research Association*


Prepared for Langley Research Center
under Contract NAS1-97046

November 2002

Available from the following:

NASA Center for AeroSpace Information (CASI)
7121 Standard Drive
Hanover, MD 21076-1320
(301) 621-0390

National Technical Information Service (NTIS)
5285 Port Royal Road
Springfield, VA 22161-2171
(703) 487-4650

# THE STRESS-STRAIN BEHAVIOR OF POLYMER-NANOTUBE COMPOSITES FROM MOLECULAR DYNAMICS SIMULATION

S. J. V. FRANKLAND[1,2], V. M. HARIK[1,2,3], G. M. ODEGARD[1,2], D. W. BRENNER[4], AND T. S. GATES[5]

**Abstract.** Stress-strain curves of polymer-carbon nanotube composites are derived from molecular dynamics simulations of a single-walled carbon nanotube embedded in polyethylene. A comparison is made between the response to mechanical loading of a composite with a long, continuous nanotube (replicated via periodic boundary conditions) and the response of a composite with a short, discontinuous nanotube. Both composites are mechanically loaded in the direction of and transverse to the NT axis. The long-nanotube composite shows an increase in the stiffness relative to the polymer and behaves anisotropically under the different loading conditions. The short-nanotube composite shows no enhancement relative to the polymer, most probably because of its low aspect ratio. The stress-strain curves are compared with rule-of-mixtures predictions.

**Key Words.** carbon nanotubes, molecular dynamics simulation, polymer composites, stress-strain

**Subject Classification.** Structures and Materials

## Nomenclature

| | |
|---|---|
| $A_1$, $A_2$, $A_3$ | - Constants for torsional potential $\phi(\theta)$ |
| $A_{cell}$ | - Cross-sectional area of unit cell |
| $E$ | - Total internal energy of solid |
| $E^{\alpha}$ | - Total internal of atom $\alpha$ |
| $f_{NT}$ | - Nanotube volume fraction |
| $f_m$ | - Polymer matrix volume fraction |
| $F_i^{\alpha\beta}$ | - $i$-component of the force between atoms $\alpha$ and $\beta$ |
| $h_{vdW}$ | - Average van der Waals separation between nanotube and matrix |
| $M^{\alpha}$ | - Mass of atom $\alpha$ |
| $S$ | - Denotes constant entropy |
| $T^{\alpha}$ | - Kinetic energy of atom $\alpha$ |
| $U^{\alpha}$ | - Potential energy of atom $\alpha$ |
| $r$ | - Magnitude of separation distance between a pair of atoms |
| $r_j^{\alpha\beta}$ | - $j$-component of the separation distance of atoms $\alpha$ and $\beta$ |
| $R_{NT}$ | - Radius of nanotube |
| $U$ | - Potential energy between a pair of atoms |
| $V$ | - Volume of solid |
| $V^{\alpha}$ | - Atomic volume of atom $\alpha$ |
| $Y_1$ | - Longitudinal elastic modulus of composite |

[1] ICASE, M/S 132C, NASA Langley Research Center, Hampton, VA 23681.

[2] This research was partially supported by the National Aeronautics and Space Administration under NASA Contract No. NAS1-97046 while S. J. V. Frankland, V. M. Harik, and G. M. Odegard were in residence at ICASE, NASA Langley Research Center, Hampton, VA 23681.

[3] Current address: Swales Aerospace, M/S 190, NASA Langley Research Center, Hampton, VA 23681.

[4] Department of Materials Science and Engineering, North Carolina State University, Raleigh, NC 27695.

[5] Mechanics and Durability Branch, NASA Langley Research Center, Hampton, VA 23681.

| | |
|---|---|
| $Y_{1NT}$ | - Elastic modulus of the nanotube |
| $Y_2$ | - Transverse elastic modulus of composite |
| $Y_{2NT}$ | - Effective transverse elastic modulus of nanotube |
| $Y_m$ | - Elastic modulus of the polymer matrix |
| $\varepsilon_{ij}$ | - Strain tensor |
| $\varepsilon_{LJ}$ | - Potential well depth |
| $\phi(\theta)$ | - Torsional potential for angle $\theta$ |
| $\Phi^{\alpha}(r)$ | - Potential energy at the atom $\alpha$ for separation distance $r$ |
| $v^{\alpha}$ | - Magnitude of the velocity of atom $\alpha$ |
| $v_i^{\alpha}$ | - $i$-component of the velocity of atom $\alpha$ |
| $\theta$ | - Torsional angle around the $CH_2$-$CH_2$ bond |
| $\sigma_{ij}$ | - Stress tensor |
| $\sigma_{LJ}$ | - Van der Waals separation distance |

1. **Introduction.** In the last few years, single-walled carbon nanotube-polymer composites have generated considerable interest in the materials research community because of their potential for large increases in strength and stiffness when compared to typical carbon-fiber-reinforced polymer composites. Even though some nanotube composite materials have been characterized experimentally [1-12], the development of these materials can be greatly facilitated by using computational methods that allow for parametric studies of the influence of material and geometry. Molecular dynamics (MD) simulations can predict the effect of mechanical loading on specific regions of polymer-nanotube (NT) composites. In this work, stress-strain curves are generated from molecular dynamics simulations of polymer-NT composites to explore the nano-structural effects on the overall mechanical properties of polymer-NT composites.

Various aspects of the mechanical reinforcement of polymers by carbon nanotubes (NT) have been addressed computationally. One example of recent work is an equivalent-continuum modeling method that was used to predict the elastic properties of two single-walled polyimide-NT composites for various NT volume fractions, lengths, and orientations [13]. At the continuum level, finite element analysis has been used to predict the macroscale effects of 'wavy' or not straight NTs [14,15]. Molecular statics simulations of the transverse mechanical properties of NT bundles have shown the strong cohesion of NTs compared to a graphite-epoxy matrix [16]. Mechanical properties of NT yarns have been predicted from the elastic constants of NT bundles [17]. Molecular modeling has predicted the adhesion between a NT and various polymer matrices [18]. Molecular dynamics simulations have predicted that the polymer-NT interface can be reinforced by covalently bonding the NT to the polymer matrix [19].

Another feature of the mechanical behavior of polymer-NT composites that can be modeled is the stress-strain relation. The stress-strain relationship provides the overall mechanical response of NT-polymer composites when subjected to mechanical loading. In the present work, stress-strain curves of two polyethylene-NT composites are generated with molecular dynamics (MD) simulations [20]. The effects of both the anisotropy of the composites when subjected to different loading conditions and of the length of the NT are explored. The first composite contains a long (infinitely long) NT, and the second composite, a short NT. Details of the composite structure and MD simulations are given in Section 2. Stress-strain curves are presented for longitudinal and transverse loading conditions of each composite (Section 5). A detailed description of the computation of stress from molecular force fields in Section 3. Comparison is made of the simulated stress-strain curves with the rule of mixtures. The relevant equations are in Section 4.

**2. Molecular Dynamics Simulations.** The unidirectional NT-polymer composites contain symmetrically placed long or short NTs as shown in Figure 1. The dashed boxes in Figure 1 enclose a representative volume element that is simulated by MD. In each composite, the NTs are sufficiently separated by polymer to prevent direct NT-NT interactions. The NT composite in Figure 1(a) contains a periodically replicated (10,10) NT which spans the length of the simulation cell. (The (n,m) notation refers to the chiral vector of the NT in terms of the primitive in-plane lattice vectors of a graphene sheet [21].) In this composite, the NT is embedded in an amorphous polyethylene (PE) matrix, which is represented by beads of united atom $-CH_2-$ units. Specifically, the PE matrix has eight chains of 1095 $-CH_2-$ units. The short-fiber composite, shown in Figure 1(b), contains a 6-nm capped (10,10) NT which is approximately half the length of the simulation cell. The NT caps each consist of one half of a $C_{240}$ molecule. In this composite, the amorphous PE matrix contains eight chains of 1420 $-CH_2-$ units. The overall dimensions for the unit-cell, or minimum image, of each composite in the MD simulation are approximately 5x5x10 nm. Periodic boundary conditions were used to replicate the cell in all three dimensions. For comparison to the NT/PE composites, an equivalent-sized block of amorphous PE without a NT was also simulated. For each structure, a PE density of 0.71 g/cm$^3$ was used.

In the MD simulation, the van der Waals interfacial interaction between the polymer and the NT was modeled with the Lennard-Jones potential [22],

$$U = 4\varepsilon_{LJ}\left(\frac{\sigma_{LJ}^{12}}{r^{12}} - \frac{\sigma_{LJ}^{6}}{r^{6}}\right) \tag{2.1}$$

where $U$ is the potential energy between a pair of atoms, $r$ is the separation distance between the pair of atoms, $\varepsilon_{LJ}$ is the potential well depth, and $\sigma_{LJ}$ is the van der Waals separation distance. For the interaction between the carbon atoms of the NT and the polymer $-CH_2-$ units, the potential was parametrized with $\varepsilon_{LJ}$=0.4492 kJ/mol and $\sigma_{LJ}$=0.3825 nm [22,23]. The PE chains were simulated with a molecular-mechanics force field adapted from Reference 23. Specifically, the $-CH_2-$ units of the PE chains were separated by bond lengths of 0.153 nm by using the SHAKE algorithm, a constraint dynamics method which constrains the bond length within a user-defined tolerance [22]. Angle bending forces were modeled with a harmonic valence-angle potential having an equilibrium angle of 112.813° and a barrier of 520 kJ/mol. A torsional potential $\phi(\theta)$ of the form

$$\phi(\theta) = A_1(1+\cos\theta) + A_2(1+\cos 2\theta) + A_3(1+\cos 3\theta) \tag{2.2}$$

was used where $\theta$ is the torsional angle around the $CH_2$-$CH_2$ bond, and $A_1$=-18.087, $A_2$=-4.88, and $A_3$=31.8 kJ/mol [23]. The Lennard-Jones potential was also used to describe non-bonding interactions between –CH2- units in either the same chain or between different chains. For these interactions, $\varepsilon_{LJ}$=0.4742 kJ/mol and $\sigma_{LJ}$=0.428 nm [23]. The NT was modeled with a many-body bond-order potential developed for carbon [24]. This carbon potential is parametrized for C-C bonds of lengths up to 0.17 nm which is within the magnitude of the strain applied to the composites in the present work.

The MD simulations were carried out by using DL-POLY [25], a large-scale MD simulation package available from Daresbury Laboratory. This program was adapted to include the carbon potential for the NT and to simulate the application of strain to the composite. All simulations were carried out at 300 K, with a 2 fs timestep.

**3. Stress-strain Curves from Simulation.** Stress-strain curves were generated for the long- and short-NT composites and for the pure polymer via MD simulation. For both composite configurations, the longitudinal (parallel to the NT axis) and transverse responses were simulated.

**3.1. Strain**. For each increment of applied deformation, a uniform strain was prescribed on the entire MD model. For the longitudinal and transverse deformations, pure states of the strains $\varepsilon_{11}$ and $\varepsilon_{22}$, respectively, were initially applied (see Figure 2). The application of strain was accomplished by uniformly expanding the dimensions of the MD cell in the direction of the deformation and re-scaling the new coordinates of the atoms to fit within the new dimensions. After this initial deformation, the MD simulation was continued and the atoms were allowed to equilibrate within the new MD cell dimensions. This process was carried out for the subsequent increments of deformation. The applied strain increment, in either the longitudinal or transverse direction, was 2%, and was applied in two increments of 1% each 1 ps (500 steps) apart. After each 2% increment of strain, the system was relaxed for 2 ps, then the stress on the system was averaged over an interval of 10 ps. For each configuration, six increments of 2 % strain were applied up to a total of approximately 12 % over a period of 72 ps. The corresponding strain rate was $1.0\text{x}10^{10}$ $s^{-1}$. This high strain rate is inherent to MD simulation which includes dynamical information usually on ps or ns timescales.

**3.2. Stress.** In general, the stress in a solid (or a group of interacting particles in the form of a solid) is defined as the change in the internal energy (in the thermodynamic sense) with respect to the strain per unit volume. For example, at the continuum level, the stress tensor for a linear-elastic material is [26]

$$\sigma_{ij} = \frac{1}{V}\left(\frac{\partial E}{\partial \varepsilon_{ij}}\right)_S \tag{3.1}$$

where $V$ is the volume of the solid, $E$ is the total internal energy, $\varepsilon_{ij}$ is the strain tensor, and the subscript $S$ denotes constant entropy. Assuming that the internal energy is equal to the strain energy of the solid, then Hooke's law may be derived from equation (3.1). Furthermore, if the strain energy is expressed in terms of an applied force acting over the surface area of a solid, then a more familiar form of stress as force per unit area is derived.

At the atomic level, the total internal energy given in equation (3.1) can be expressed as the summation of the energies of the individual atoms, $E^\alpha$, that compose the solid:

$$E^\alpha = T^\alpha + U^\alpha = \frac{1}{2}M^\alpha\left(v^\alpha\right)^2 + \Phi^\alpha\left(r\right) \tag{3.2}$$

where for each atom $\alpha$, $T^\alpha$ is the kinetic energy, $U^\alpha$ is the potential energy, $M^\alpha$ is the mass, $v^\alpha$ is the magnitude of its velocity, and $\Phi^\alpha(r)$ is the potential energy at the atom location $r$. Using a Hamiltonian based on these individual energy contributions, $E^\alpha$, it has been shown that the stress contribution for a given atom is

$$\sigma_{ij}^\alpha = -\frac{1}{V^\alpha}\left(M^\alpha v_i^\alpha v_j^\alpha + \sum_\beta F_i^{\alpha\beta} r_j^{\alpha\beta}\right) \tag{3.3}$$

where $V^\alpha$ is the atomic volume of atom $\alpha$, $v_i^\alpha$ is the $i$-component of the velocity of atom $\alpha$, $v_j^\alpha$, is the $j$-component of the velocity of atom $\alpha$, $F_i^{\alpha\beta}$ is the $i$-component of the force between atoms $\alpha$ and $\beta$ obtainable from the derivative of the potential $\Phi(r)$, and $r_j^{\alpha\beta}$ is the $j$-component of the separation of atoms $\alpha$ and $\beta$ (Figure 3) [27,28].

The stresses that were used to generate the stress-strain curves for the NT composite were average atomic stresses for the volume of the model. Therefore, the stress components of each model were calculated for each strain increment by using

$$\sigma_{ij} = -\frac{1}{V}\sum_\alpha\left(M^\alpha v_i^\alpha v_j^\alpha + \sum_\beta F_i^{\alpha\beta} r_j^{\alpha\beta}\right) \tag{3.4}$$

where $V$ is the volume of the MD model and $V = \sum_{\alpha} V^{\alpha}$. The stress calculated with equation (3.4) was then averaged over time via the MD simulation.

**4. Rule-of-Mixture Analysis.** For a nanocomposite under uniaxial loading, the dependence of the elastic modulus on the NT volume fraction can be estimated by the rule of mixtures [29]. The longitudinal elastic modulus, $Y_1$, of the composite cell with long NTs under isostrain conditions is

$$Y_1 = Y_{1NT} f_{NT} + Y_m f_m \tag{4.1}$$

where $Y_{1NT}$ and $Y_m$ are the effective longitudinal elastic modulus of the NT and the polymer matrix, respectively, and $f_{NT}$ and $f_m$ are the volume fractions occupied by the NT and the polymer matrix, respectively. The transverse modulus of the nanocomposite, $Y_2$, is

$$\frac{1}{Y_2} = \frac{f_{NT}}{Y_{2NT}} + \frac{f_m}{Y_m} \tag{4.2}$$

where $Y_{2NT}$ is the effective elastic modulus of a NT in the transverse direction. The volume fractions satisfy

$$f_{NT} + f_m = 1. \tag{4.3}$$

The (10,10) NT used in the present work has a radius small enough to be thought of as a solid beam [30]. Therefore, its volume fraction, $f_{NT}$, includes the entire NT cross-section and is given by $\pi(R_{NT}+h_{vdW}/2)^2/A_{cell}$, where $h_{vdW}$ is the equilibrium van der Waals separation distance between the NT and the matrix, and $A_{cell}$ is the cross-sectional area of the unit cell. The van der Waals separation distance depends on the nature of the polymer/NT interfacial interactions.

**5. Results and Discussion.** The stress-strain curves of the long- and short-NT composites generated from MD simulation are presented in Figures 4, 5, and 6. Before describing the individual stress-strain curves in more detail, some general comments are in order. First, the endpoints of the curves are indicative of how far the simulation was run, and hence, should not be taken as yield points. No attempt is made in this work to simulate the yielding of carbon nanotubes. Also, for both composite configurations, the maximum strains are on the order of 10 % after the unit cell had been subjected to stepwise increases of applied strain. The strain leads to an overall displacement of 0.5 nm for each unit-cell edge in the longitudinal direction and 0.25 nm in the transverse direction.

In Figure 4, the stress-strain curve (solid triangles on solid line) of the long-NT composite under longitudinal loading conditions is compared with the rule of mixtures (solid line without symbols) from equation (4.1). Of the composites simulated here, this one has the most significant enhancement in its stress-strain curve relative to the polymer (to be shown in Figure 5). For this sample, both the NT and the polymer were subjected to constant strain conditions. The stress-strain curve is comparable at low strain to the stress-strain behavior predicted by the rule of mixtures in equation (4.1) using a volume fraction of 8%, which is the NT volume fraction in the simulated composite, and an effective modulus of 600 GPa for the (10,10) NT [31].

The stress-strain curve of the short-NT (solid circles on solid line) subjected to longitudinal loading conditions is plotted with the simulated polymer stress-strain curve (solid squares on solid line) in Figure 5. Almost no enhancement relative to the polymer is observed in the stress-strain curve of the

composite with the short 6-nm NT. The bulk polymer stiffness is improved by less than a factor of two when the NTs are added into the polymer. This lack of effect is consistent with the low aspect ratio of the nanotube, 1:4, which is considerably lower than the more than 1:1000 aspect ratio expected for a typical single-walled NT. Length scales of this magnitude are not accessible with the current MD simulation. Furthermore, the simulated interface is established by non-bonding van der Waals forces between the polymer and the carbon NT [32], and there are no chemical bonds [19] or other strong interactions [13] to strengthen the interfacial adhesion.

The stress-strain curves of both composites subjected to transverse loading conditions are compared with each other and the polymer (solid circles on solid line) in Figure 6. All three MD generated curves are similar. For the composite with the long NT (solid squares on solid line), the stress after loading in the transverse direction is approximately 30 times lower than the stress levels after loading to the same strain level in the longitudinal direction (Figure 4). This difference in longitudinal and transverse behavior emphasizes the anisotropy of the composite. Both the long- and short-NT composites have more similar transverse behavior than the polymer which may be because the NT fills the same relative cross-sectional area in both composites. The solid line in Figure 6 is from the transverse rule of mixtures given by equation (4.2) for transverse loading conditions of the long-NT composite. For this comparison, an effective NT transverse modulus of 10 GPa [33] is used, and a polymer modulus of 2.7 GPa, which is derived from the initial points of the simulated polymer stress-strain curve. For somewhat higher estimates of the NT transverse modulus, the predictions will not change because the contribution from the matrix modulus is dominant in equation (4.2).

**6. Concluding Remarks**. Molecular dynamics (MD) simulations were used to establish the stress-strain behavior of polymer-carbon nanotube (NT) composites mechanically loaded in both the longitudinal and transverse directions. Two NT geometries, long continuous fibers and short discontinuous fibers were investigated. Stress at the atomic level was defined by using energy considerations, averaged over the volume of the MD model. The simulated stress-strain curves were compared with the rule of mixtures.

The stiffest behavior, and the one closest to approaching the rule of mixtures, was observed for the longitudinally loaded, long continuous NT composite. This composite was very anisotropic showing stresses that, when subjected to transverse loading conditions, were more than one order of magnitude lower than when subjected to longitudinal loading conditions. By contrast, the short, discontinuous fiber composite, upon loading in either direction, showed no appreciable load transfer from the polymer to the NT. It is anticipated that increasing the aspect ratio of NT in this composite would lead to further enhancement of the stress-strain curve and greater differences between the longitudinal and transverse stress-strain behavior [19,34].

**Acknowledgment.** Support from a Multi-University Research Initiative of the Office of Naval Research through the North Carolina Center for Nanoscale Materials is gratefully acknowledged by S. J. V. Frankland and D. W. Brenner. The simulations were carried out with facilities at the North Carolina Supercomputing Center.

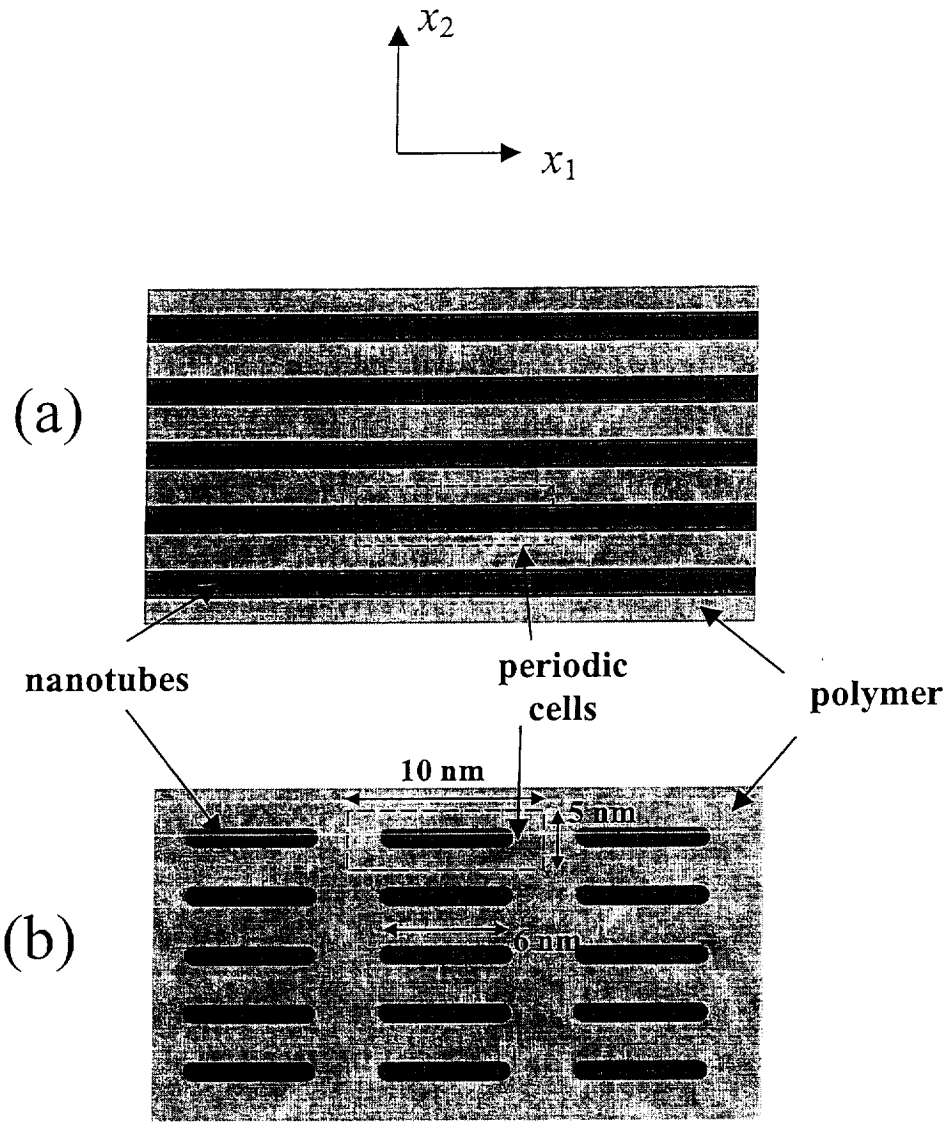


FIG. 1. *Schematic of polymer nanocomposites filled with long and short carbon nanotubes*

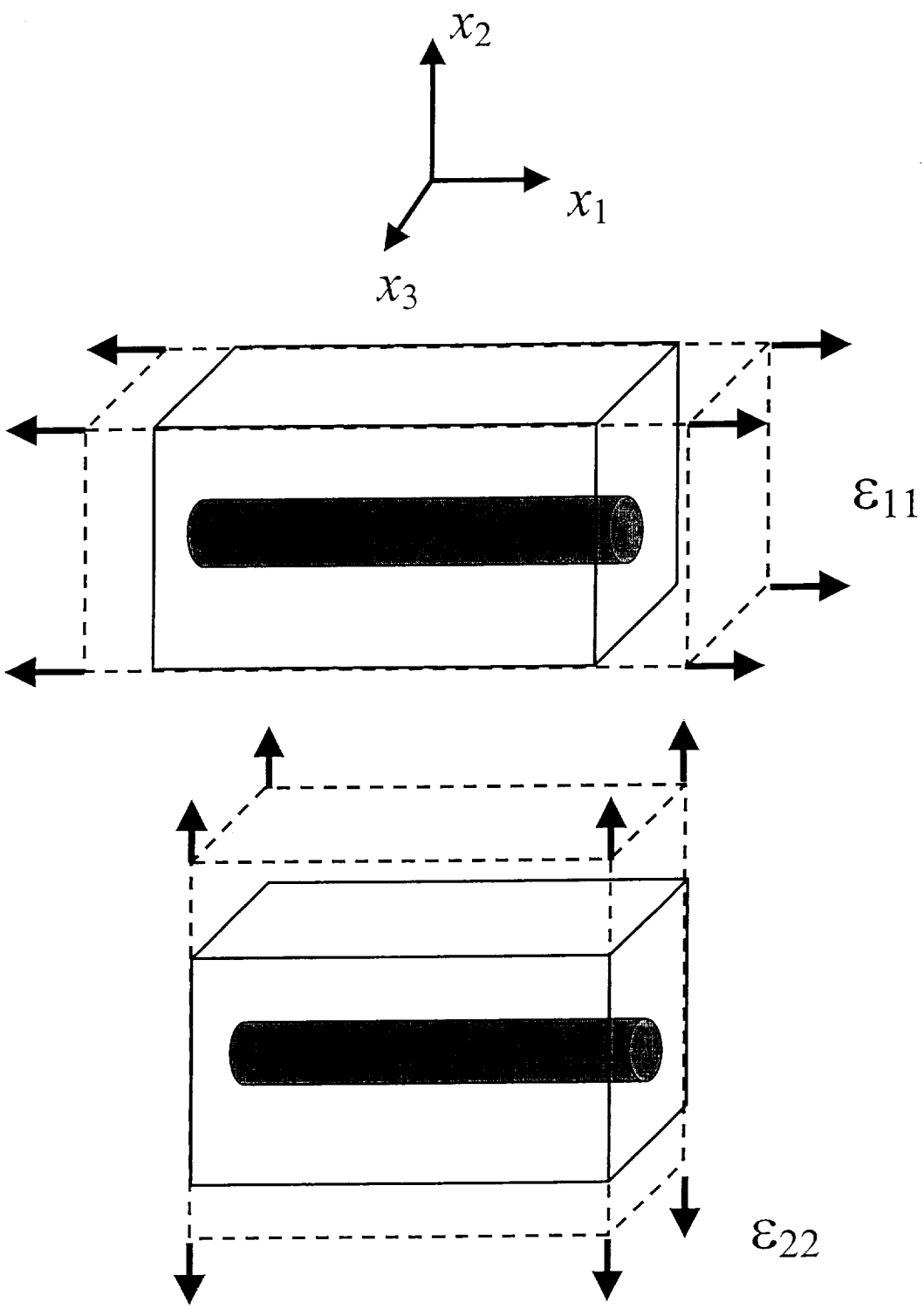


FIG. 2. *Definitions of the strains applied to the composites*

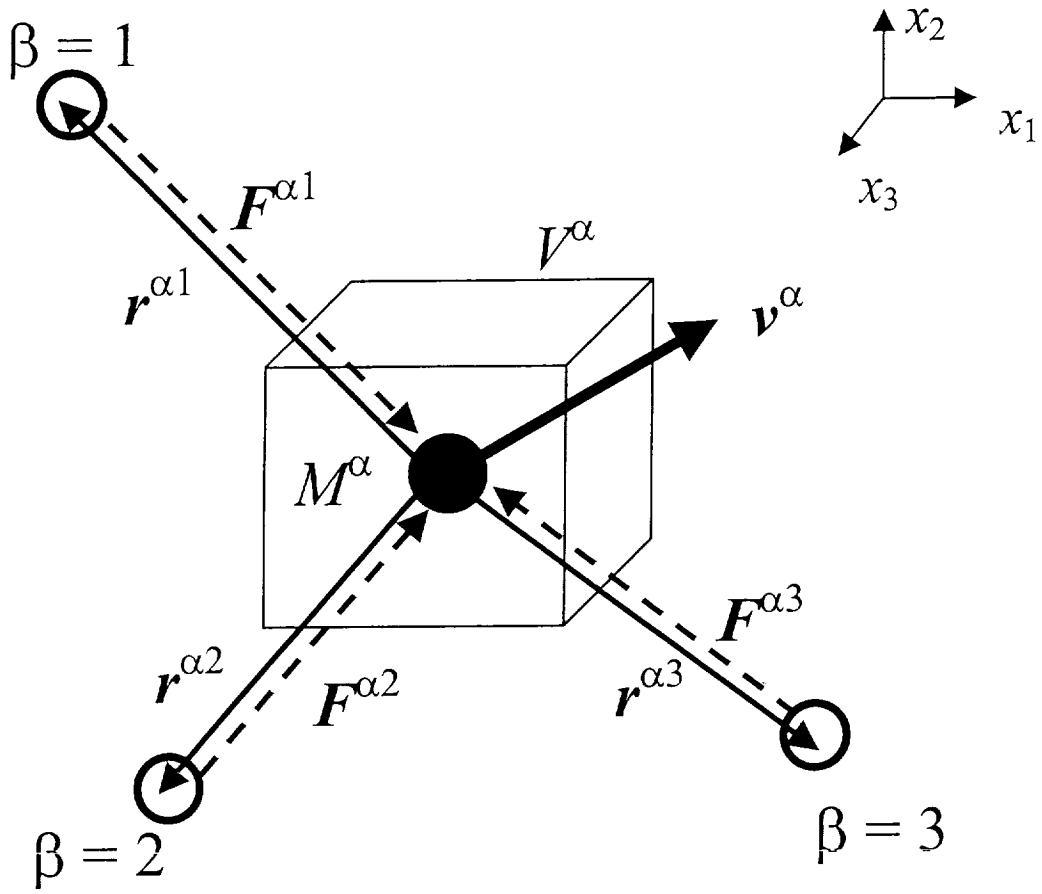


FIG. 3. *Diagram of parameters used to compute stresses in the simulation (see text for details)*

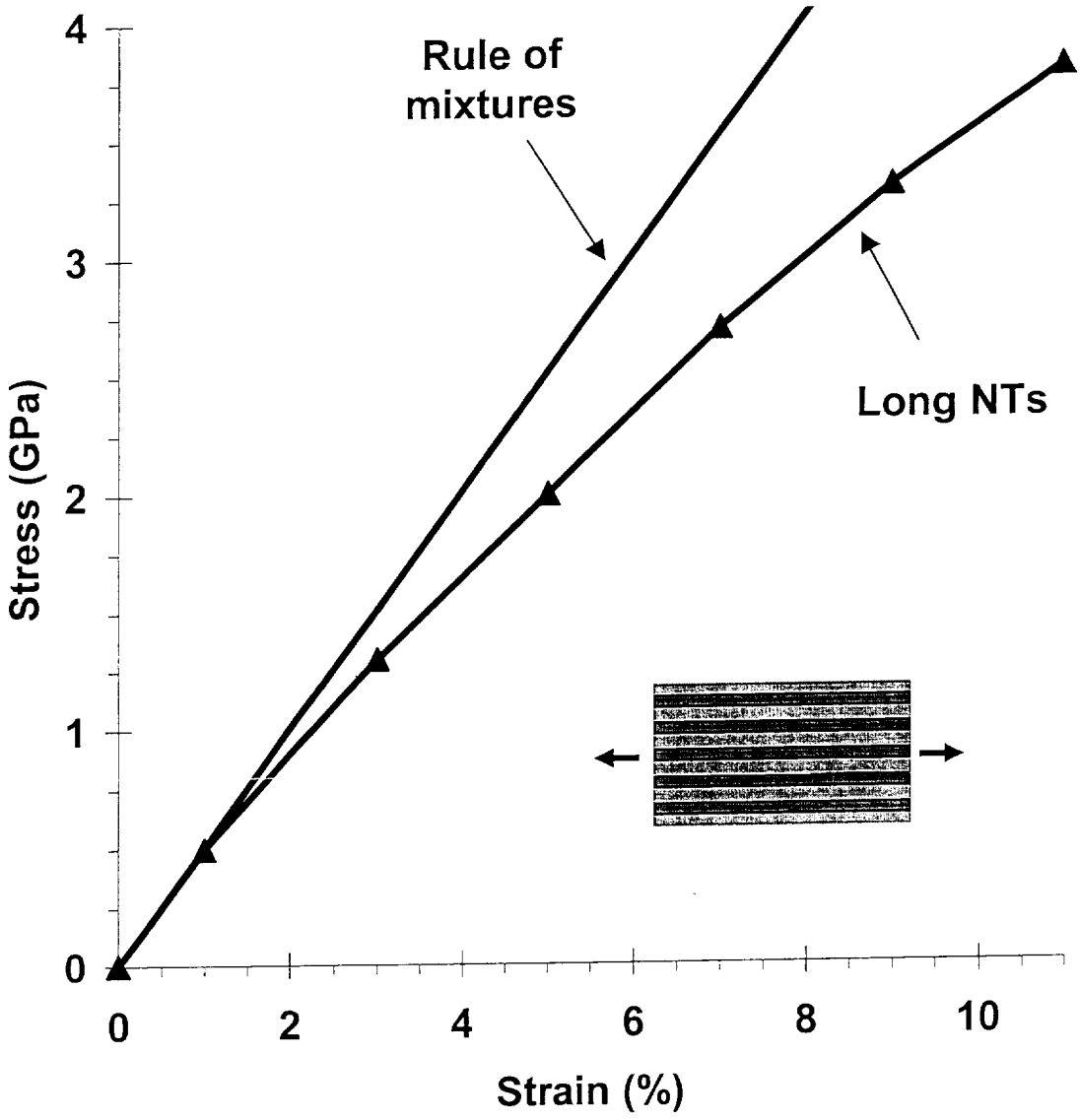


FIG. 4. *Longitudinal stress-strain relation of long-NT composite and comparison to rule of mixtures*

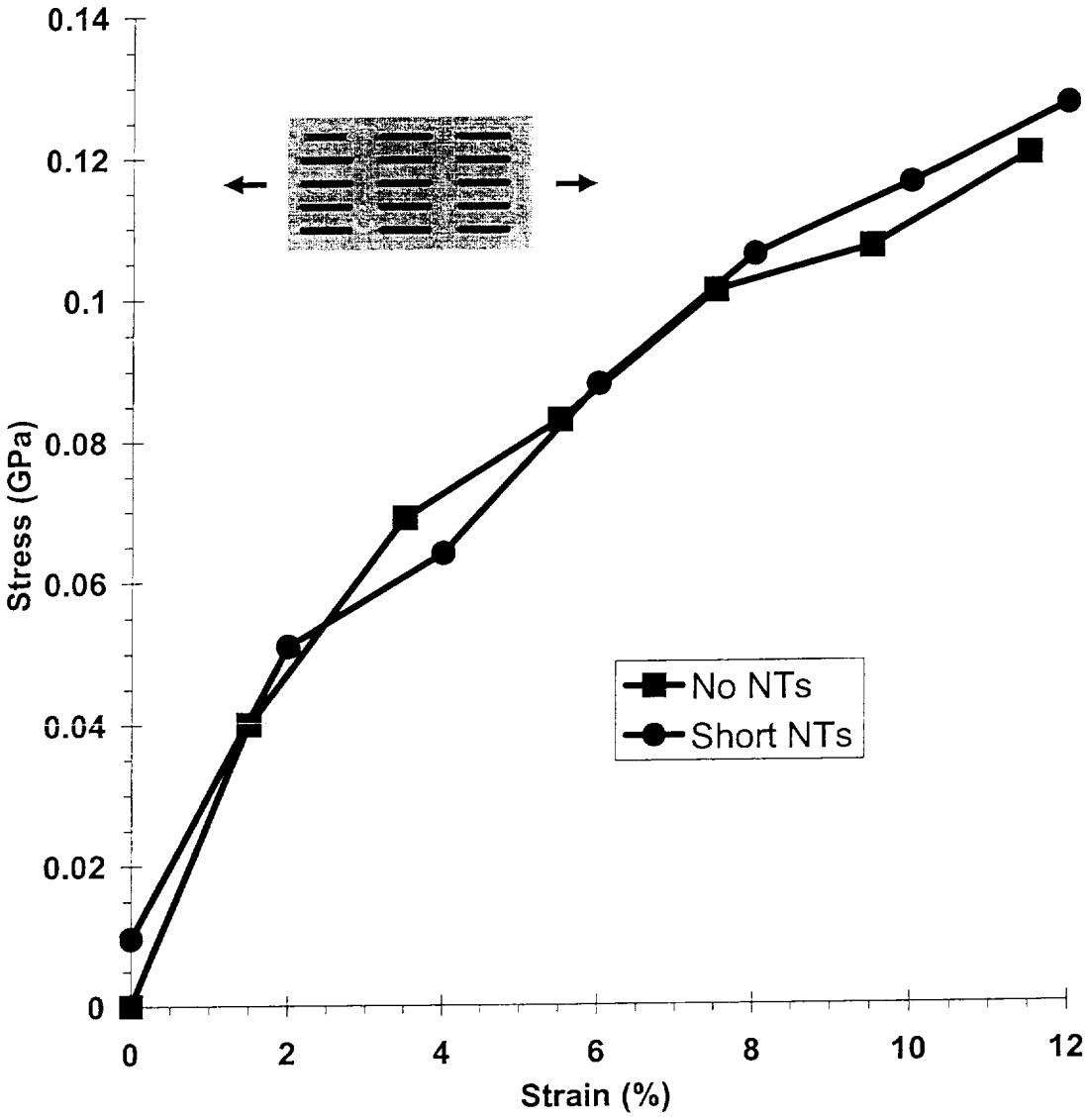


FIG. 5. *Longitudinal stress-strain relation for short NT composite compared with the stress-strain behavior of the polymer matrix and the rule of mixtures for transverse modulus*

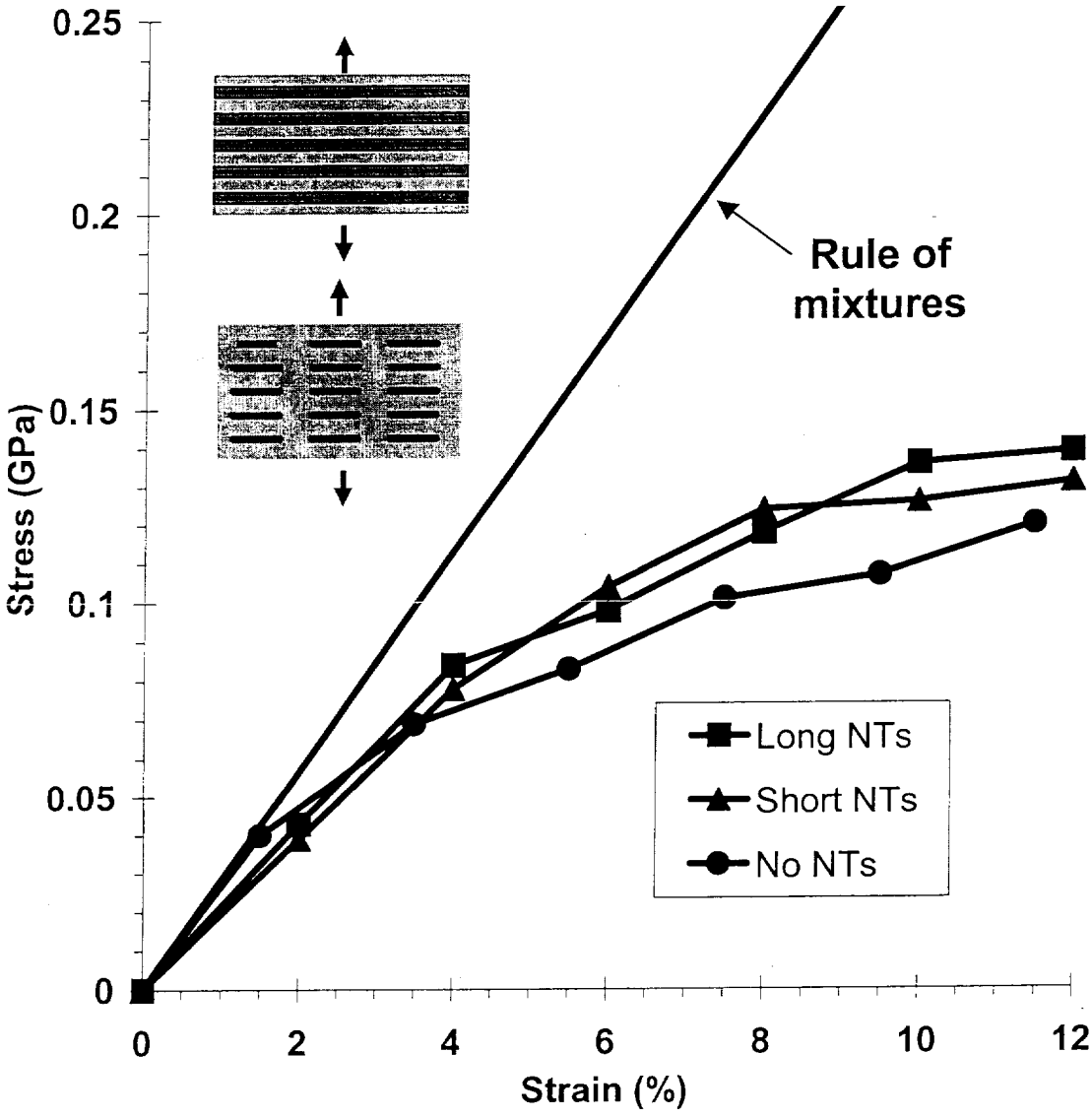


FIG. 6. *Transverse stress-strain curves of both long and short NT-filled composites compared with polymer matrix and the transverse rule of mixtures for the long NT-filled composite*

## REFERENCES


[1] L. S. SCHADLER, S. C. GIANNARIS, and P. M. AJAYAN, *Load transfer in carbon nanotube epoxy composites*, Appl. Phys. Lett., 73 (1998) pp. 3842-3844.

[2 ] P. M. AJAYAN, L. S. SCHADLER, S. C. GIANNARIS, and A. RUBIO, *Single-walled carbon nanotube-polymer composites: Strength and weakness*, Adv. Materials, 12 (2000) pp. 750-753.

[3] X. GONG. J. LIU, S. BASKARAN, R. D. VOISE, and J. S. YOUNG, *Surfactant-assisted processing of carbon nanotube/polymer composite,* Chem. Mater., 12 (2000) pp. 1049-1052.

[4] R. HAGGENMUELLER, H. H. GOMMANS, A. G. RINZLER, J. E. FISCHER, and K. I. WINEY, *Aligned single-wall carbon nanotubes in composites by melt processing methods*, Chem. Phys. Lett., 330 (2000) pp. 219-225.

[5] D. QIAN, E. C. DICKEY, R. ANDREWS, and T. RANTELL, *Load transfer and deformation mechanisms in carbon nanotube-polystyrene composites,* Appl. Phys. Lett., 76 (2000) pp. 2868-2870.

[6] M. S. P. SHAFFER, and A. H. WINDLE, *Fabrication and characterization of carbon nanotube/poly(vinyl alcohol) composites*, Adv. Materials, 11 (1999) pp. 937-941.

[7] L. JIN, C. BOWER, and O. ZHOU, *Alignment of carbon nanotubes in a polymer matrix by mechanical stretching*, Appl. Phys. Lett., 73 (1998) pp. 1197-1199.

[8] C. BOWER, R. ROSEN, L. JIN, J. HAN, and O. ZHOU, *Deformation of carbon nanotubes in nanotube-polymer composites,* Appl. Phys. Lett., 74 (1999) pp. 3317-3319.

[9] H. D. WAGNER, O. LOURIE, Y. FELDMAN, and R. TENNE, *Stress-induced fragmentation of multiwall carbon nanotubes in a polymer matrix,* Appl. Phys. Lett., 72 (1998) pp. 188-190.

[10] O. LOURIE and H. D. WAGNER, *Transmission electron microscopy observations fracture of single-wall carbon nanotubes under axial tension*, Appl. Phys. Lett., 73 (1998) pp. 3527-3529.

[11] M. LAMY DE LA CHAPELLE, C. STEPHAN, T. P. NGUYEN, S. LEFRANT, C. JOURNET, P. BERNIER, E. MUNOZ, A. BENITO, W. K. MASER, M. T. MARTINEZ, G. D. DE LA FUENTE, T. GUILLARD, G. FLAMANT, L. ALVAREZ, and D. LAPLAZE, *Raman characterization of singlewalled carbon nanotubes and PMMA-nanotubes composites,* Synthetic Metals, 103 (1999) pp. 2510-2512.

[12] Z. JIA, Z. WANG, C. XU, J. LIANG, B. WEI, D. WU, and S. ZHU, *Study on poly(methyl methacrylate)/carbon nanotube composites,* Mat. Sci. Eng. A, 271 (1999) pp. 395-400.

[13] G. M. ODEGARD, T. S. GATES, K. WISE, C. PARK, and E. J. SIOCHI, *Constitutive modeling of nanotube reinforced polymer composites*, Composites Science and Technology; to be submitted to this issue.

[14] F. T. FISHER, R. D. BRADSHAW, and L. C. BRINSON, *Fiber waviness in nanotube-reinforced polymer composites: I. Modulus predictions using effective Nanotube properties*, Composites Science and Technology; to be submitted to this issue.

[15 ] R. D. BRADSHAW, F. T. FISHER, and L. C. BRINSON, *Fiber waviness in nanotube-reinforced polymer composites II. Modeling via numerical approximation of the dilute strain concentration tensor,* Composites Science and Technology; to be submitted to this issue.

[16] E. SAETHER, S. J. V. FRANKLAND, and R. B. PIPES, *Transverse mechanical properties of single-walled carbon nanotube crystals,* Composites Science and Technology; to be submitted to this issue.

[17] R. B. PIPES and P. HUBERT, *Helical carbon nanotube arrays: Mechanical properties*, Comp. Science and Technology, 62 (2002) pp. 419-428.

[18] V. LORDI and N.YAO, *Molecular mechanics of binding in carbon nanotube–polymer composites,* J Mater. Res., 15 (2000) pp. 2770-2779.

[19] S. J. V. FRANKLAND, A. CAGLAR, D. W. BRENNER, and M. GRIEBEL, *Molecular simulation of the influence of chemical cross-links on the shear strength of carbon nanotube-polymer interfaces*, J. Phys. Chem. B, 106 (2002) pp. 3046-3049.

[20] S. J. V. FRANKLAND and D. W. BRENNER, *Molecular dynamics simulations of polymer-nanotube composites*, in Amorphous and Nanostructured Carbon, J. P. Sullivan, J. Robertson, O. Zhou, T. B. Allen, and B. F. Coll, editors, (Mat. Res. Soc. Symp. Proc., 593, Warrendale, PA, 1999) pp. 199-204.
[21] M. S. DRESSELHAUS, G. DRESSELHAUS, and P. C. EKLUND, Science of Fullerenes and Carbon Nanotubes, Academic Press, Inc, New York, 1996.
[22] M. P. ALLEN and D. J. TILDESLEY, *Computer Simulation of Liquids*, Clarendon Press, Oxford, 1987.
[23] J. H. R. CLARKE, in Monte Carlo and Molecular Dynamics in Polymer Sciences, K. Binder, ed., Oxford University Press, New York, 1995, p. 272.
[24] D. W. BRENNER, O. A. SHENDEROVA, J. A. HARRISON, S. J. STUART, B. NI, and S. B. SINNOTT, *Second generation reactive empirical bond order (REBO) potential energy expression for hydrocarbons,* J. Phys C: Condensed Matter, 14 (2002) pp. 783.
[25] DL-POLY is a package of molecular simulations subroutines written by W. Smith and T. R. Forester, copyright The Council for the Central Laboratory of the Research Councils, Daresbury Laboratory at Daresbury, Nr. Warrington, England, UK, 1996.
[26] C. Y. FUNG, *Foundations of Solid Mechanics*, Prentice-Hall, Inc., Englewood Cliffs, NJ, 1965.
[27] O. H. NIELSEN and R. M. MARTIN, *Quantum-mechanical theory of stress and force,* Physical Review B, 32 (1985) pp. 3780-3791.
[28] V. VITEK and T. EGAMI, *Atomic level stresses in solids and liquids,* Physica Status Solidi. B: Basic Research, 144 (1987) pp. 145-156.
[29] S. W. TSAI, *Composites Design*, Think Composites Press, Dayton, OH, 1988.
[30] V. M. HARIK, *Ranges of applicability for the continuum beam model in mechanics of carbon nanotubes and nanorods*, Solid State Commun., 120 (2001) pp. 331-335.
[31] C. F. CORNWELL and L. T. WILLE. *Elastic properties of single-walled carbon nanotubes in compression*, Solid State Commun., 101 (1997) pp. 555-558.
[32] S. J. V. FRANKLAND, A. CAGLAR, D. W. BRENNER, and M. GRIEBEL, *Reinforcement mechanisms in polymer nanotube composites: Simulated non-bonded and cross-linked systems,* Mat. Res. Soc. Symp. Proc., 633 (2000) pp. A.14.17.1-5.
[33] V. N. POPOV, V. E. VAN DOREN, and M. BALKANSKI, *Elastic properties of crystals of single-walled carbon nanotubes,* Solid State Commun., 114 (2000) pp. 395-399.
[34] A. KELLY and N. H. MACMILLAN, *Strong Solids*, 3rd ed., Clarendon Press, Oxford, 1986.

# REPORT DOCUMENTATION PAGE

*Form Approved*
*OMB No. 0704-0188*

Public reporting burden for this collection of information is estimated to average 1 hour per response, including the time for reviewing instructions, searching existing data sources, gathering and maintaining the data needed, and completing and reviewing the collection of information. Send comments regarding this burden estimate or any other aspect of this collection of information, including suggestions for reducing this burden, to Washington Headquarters Services, Directorate for Information Operations and Reports, 1215 Jefferson Davis Highway, Suite 1204, Arlington, VA 22202-4302, and to the Office of Management and Budget, Paperwork Reduction Project (0704-0188), Washington, DC 20503.

| 1. AGENCY USE ONLY *(Leave blank)* | 2. REPORT DATE | 3. REPORT TYPE AND DATES COVERED |
|---|---|---|
| | November 2002 | Contractor Report |

**4. TITLE AND SUBTITLE**
THE STRESS-STRAIN BEHAVIOR OF POLYMER-NANOTUBE COMPOSITES FROM MOLECULAR DYNAMICS SIMULATION

**5. FUNDING NUMBERS**
C NAS1-97046
WU 505-90-52-01

**6. AUTHOR(S)**
S.J.V. Frankland, V.M. Harik, G.M. Odegard, D.W. Brenner, and T.S. Gates

**7. PERFORMING ORGANIZATION NAME(S) AND ADDRESS(ES)**
ICASE
Mail Stop 132C
NASA Langley Research Center
Hampton, VA 23681-2199

**8. PERFORMING ORGANIZATION REPORT NUMBER**
ICASE Report No. 2002-41

**9. SPONSORING/MONITORING AGENCY NAME(S) AND ADDRESS(ES)**
National Aeronautics and Space Administration
Langley Research Center
Hampton, VA 23681-2199

**10. SPONSORING/MONITORING AGENCY REPORT NUMBER**
NASA/CR-2002-211953
ICASE Report No. 2002-41

**11. SUPPLEMENTARY NOTES**
Langley Technical Monitor: Dennis M. Bushnell
Final Report
To be submitted to Composite Science and Technology.

**12a. DISTRIBUTION/AVAILABILITY STATEMENT**
Unclassified–Unlimited
Subject Category 34
Distribution: Nonstandard
Availability: NASA-CASI (301) 621-0390

**12b. DISTRIBUTION CODE**

**13. ABSTRACT** *(Maximum 200 words)*

Stress-strain curves of polymer-carbon nanotube composites are derived from molecular dynamics simulations of a single-walled carbon nanotube embedded in polyethylene. A comparison is made between the response to mechanical loading of a composite with a long, continuous nanotube (replicated via periodic boundary conditions) and the response of a composite with a short, discontinuous nanotube. Both composites are mechanically loaded in the direction of and transverse to the NT axis. The long-nanotube composite shows an increase in the stiffness relative to the polymer and behaves anisotropically under the different loading conditions. The short-nanotube composite shows no enhancement relative to the polymer, most probably because of its low aspect ratio. The stress-strain curves are compared with rule-of-mixtures predictions.

| 14. SUBJECT TERMS | 15. NUMBER OF PAGES |
|---|---|
| carbon nanotubes, molecular dynamics simulation, polymer composites, stress-strain | 19 |
| | 16. PRICE CODE: A03 |

| 17. SECURITY CLASSIFICATION OF REPORT | 18. SECURITY CLASSIFICATION OF THIS PAGE | 19. SECURITY CLASSIFICATION OF ABSTRACT | 20. LIMITATION OF ABSTRACT |
|---|---|---|---|
| Unclassified | Unclassified | | |